DOI 10.7251/JEPM1709081K
UDC 542.943:546.831

Journal of
Engineering & Processing
Management

ORIGINAL SCIENTIFIC PAPER

Air-thermal oxidation of zirconium

Zagorka Koneska | Ružica Manojlović | Dafinka Stoevska-Gogovska

University "Ss Cyril and Methodius", Faculty of Technology and Metallurgy, 1000 Skopje, Republic of Macedonia.

Correspodence:
Zagorka Koneska, University "Ss Cyril and Methodius", Faculty of Technology and Metallurgy, Skopje, Republic of Macedonia.

Email: zaga@tmf.ukim.edu.mk

Key words:
corrosion, thermal oxidation, zirconium, ZrO_2*.*

Abstract

Zirconium is one of those few metals which are capable of dissolving relatively large quantities of oxygen. When heated in air at elevated temperatures, an oxide layer is built up at the metal surface. The oxidation of mechanically polished zirconium was studied in the range 500-900oC in air atmosphere, at temperature intervals of 100oC, for exposure times from 5 min to 1860 min for each temperature. The weight gain of the oxidized species was the reacted amount of oxygen with zirconium for the formation of the ZrO2. The weight gain and thickness of the oxide film increase with the increasing of the oxidation time and temperature. The oxidation initially followed a parabolic rate at all temperatures. At temperatures higher than 700oC oxide "breakaway" appears at the longest oxidation times. Microstructural investigations have shown that the oxide layers are compact and with good adhesion to the metal surface, but at temperatures over 700oC, radial micro-cracks appear. Raman spectra of the formed oxides at the investigated temperatures are characteristic for monoclinic phase.

1. INTRODUCTION

The reaction of metal surface with oxygen is one of the reactions that cause great interest, due to the importance of its application areas: catalysis, microelectronics, surface coatings and corrosion protection. Oxidation of metals is often associated with corrosion, which causes undesired destruction and loss of metal.

Elements such as Zr, Ti and Nb, which belong to a group known as valve metals, usually have their surfaces covered with a thin oxide film, spontaneously formed in air or in electrolytes at open circuit potential.

The presence of a thin oxide film on the surface of a pure metal or alloy substrate has a direct bearing to a variety of its chemical and physical properties. This film provides a barrier between the metal and the medium. Typical values of the initial thickness of these oxide films are in the range of 2-5 nm, when formed in air at room temperature, but the thickness of the films can be increased by thermal oxidation or by anodic oxidation [1].

Oxide materials have an abundance of interesting physical properties that can be used for various technological applications. Many oxide materials have been used extensively in the form of thin films because the applications involve micro-devices that require materials fabricated on micron or submicron scales [2].

Both zirconium and zirconium oxide are material with significant technological importance. Due to their specific physical and chemical properties, they are widely used in a large number of application areas.

ZrO_2 is a material with particular technological importance, considering it has good natural colour, high strength, transformation toughness, high chemical stability, excellent corrosion, chemical and microbial resistance [3, 4, 5].

ZrO_2 is a wide band gap p-type semiconductor that exhibits abundant oxygen vacancies on its surface. The high ion exchange capacity and redox activities make it especially useful in catalysis [6]. ZrO_2 is also an important dielectric material for potential application as an insulator in transistors in future nanoelectric devices [7]. Garcia et al. have highlighted its potential to replace SiO_2 in advanced metal oxide semiconductor (MOS) devices and in optical applications [8]. ZrO_2 nanoparticles have found uses in solid oxide fuel cells [9].

Thermal oxidation of zirconium alloys has been studied for a long time and a significant understanding of the processes for high temperature conditions in oxidizing environments has been achieved [10]. However, discussion about the role of various processes that affect the growth rate of oxide films and corrosion regimes still continues.

2. EXPERIMENTAL

The samples studied in this work were rods of polycrystalline zirconium purchased from Alfa with defined surfaces.

The chemical composition of the specimen (wt%) is presented in Table 1.

Table1. Chemical composition of the specimen

Hf	Fe+Cr	N	O	H	C	Zr
1	0.08	0.005	0.16	0.0003	0.02	balance

After abrasion with emery paper, the samples were polished on metallurgical cloths with diamond paste of 9 and 3 □m. The polishing with 3 □m diamond paste left a mirror-like finish of the surface. Then, the samples were subjected to ultrasonic cleaning.

After polishing, cleaning and drying, the samples were oxidized in a furnace, type Heraeus, at different temperatures for different time in the air atmosphere.

The mass of samples before and after the oxidation was measured using high-precision Mettler balance.

The structure of the thermally formed zirconium oxides were studied by means of metallography and Raman spectroscopy. The metallographic microscope type Neophot 2 and Renishaw Ramascope with red laser 632.8 nm and power of 1 MW, were used in the investigations.

Figure 1 represents the micrograph of the initial zirconium surface after cleaning [11].

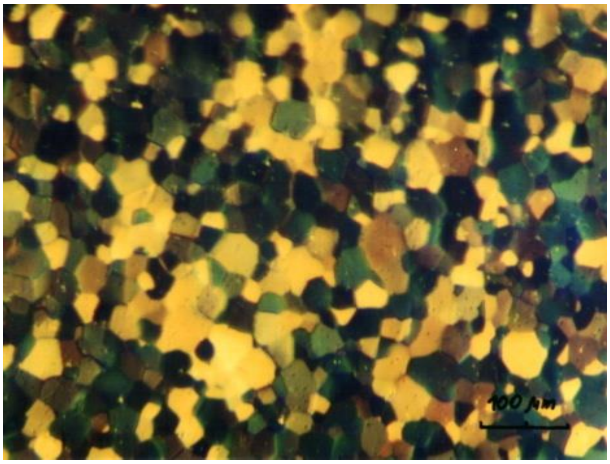

Figure 1. The micrograph of the initial zirconium surface (polarized light mode)

The zirconium specimens were oxidized in air atmosphere, at a temperature interval of 100oC, over the range 500-900oC. The oxidation period varied from 5 to 1860 min for each temperature.

3. RESULTS

Measurements of the sample weight gains against the oxidation periods at temperatures in the range 500-900oC are represented by the curves in Figure 2. As can be seen from the curves, increasing of the oxidation time increases the weight gain of the samples for all temperatures.

The logarithms of the weight gain during the air oxidation are plotted against the logarithms of oxidation periods at various temperatures in Figure 3.

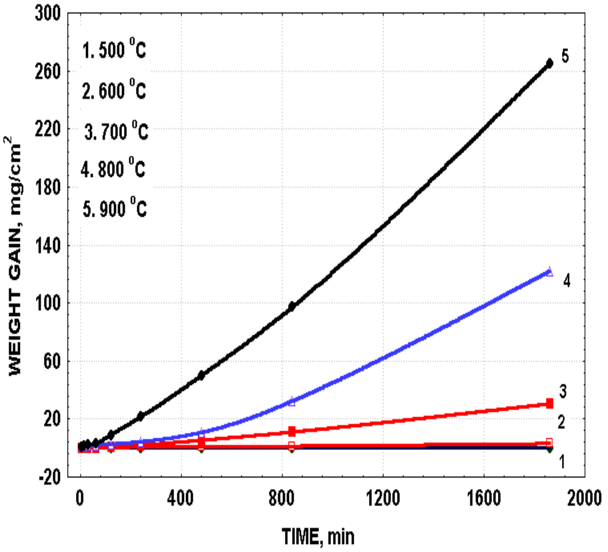

Figure 2.Oxidation weight gain of Zr in air

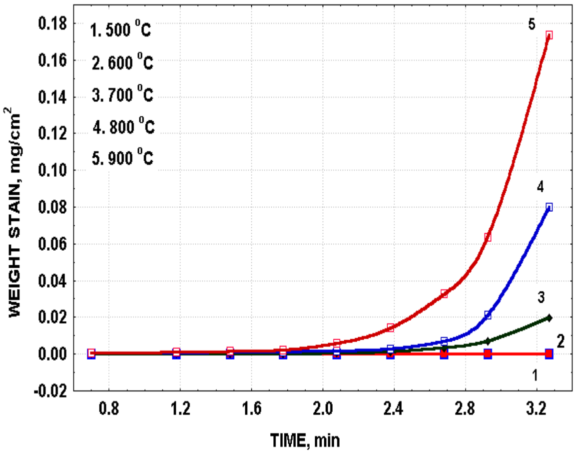

Figure 3. Log weight gain – log time curves at investigated temperatures

The plots show that oxidation initially follows a parabolic rate at all temperatures. A significant breakaway phenomenon in the oxidation rate was observed in the temperature region above 700oC. In this temperature region, the oxidation kinetics changed, from an initial parabolic to a faster linear rate. It can be noted that for temperature of 900oC breakaway occurred in an early stage, approximately 230 min after the start of oxidation, compared with approximately 500 min at 800oC and 830 min at 700oC.

The increase of the oxidation rate which was observed at the breakaway can be due to the ingress of the oxidant down the cracks in the oxide, which then leads to a rapid oxidation.

The growth of the oxide followed a similar pattern for all temperatures, starting with of a layer of dense, black oxide on the surface. Before the breakaway, the air oxidation is controlled by the following exothermic reaction: $Zr + O_2 \rightarrow ZrO_2$ with a reaction enthalpy of $\Delta H = -1100$ kJ/mol at 298 K.

The air oxidation is controlled by a diffusion process, which can be divided in different steps: adsorption and dissociation of oxygen at the metal-atmosphere interface, oxygen diffusion/dissolving in the metal until saturation, which leads to the formation of an oxide layer, oxygen diffusion through the oxide layer and oxide growth at the metal-oxide interface [12, 13].

After the breakaway, the colour of the formed oxide varied from grey to pink and, during long exposure, it was invariable pink.

Using a parabolic relationship for the oxide formation the rate constant, Kp, was calculated. The obtained results were plotted against 1/T and the activation energy of the oxidation reaction, 129.5 kJ/mol was calculated; it is presented on Figure 4.

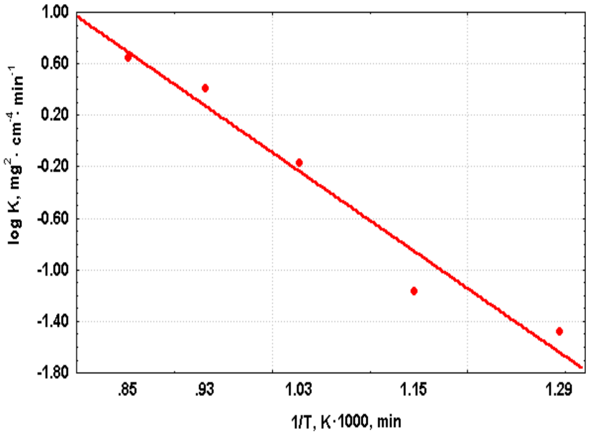

Figure 4. Arrhenius diagram for the oxidation process of Zr

Using the weight gains of the specimen oxidized at different temperatures, the corrosion rates were calculated.

In order to represent the differences before and after breakaway more clearly (the oxide layer loses its protectiveness), the corrosion rates as a function of the time are shown only for 600oC and 800oC (Figure 5).

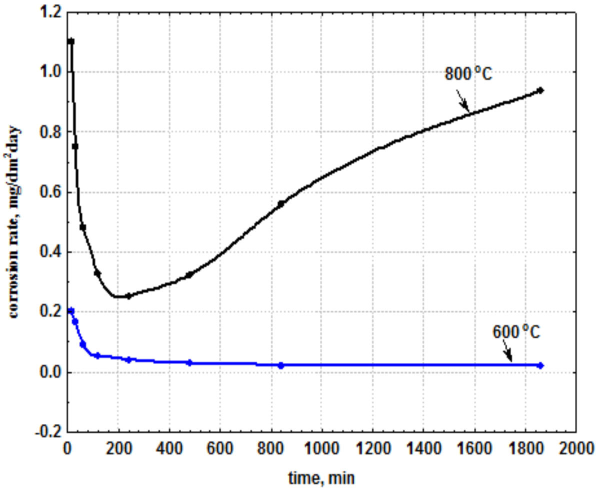

Figure 5. Corrosion rate as a function of the time

During the first 200 minutes, the corrosion rate for all species decreases. Afterwards, the corrosion rate for the samples heated at temperatures from 500 to 700°C remains almost constant, whereas for the specimens heated at 800 and 900°C after 200 minutes the corrosion rate rapidly increases. The increase of the corrosion rate at higher temperatures, at constant times, is presented in Figure 6. At temperatures below 700°C the corrosion rate is almost constant and rapidly increases at 800 and 900°C.

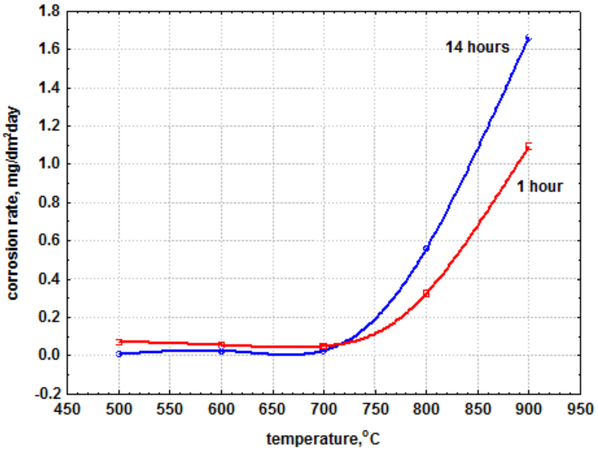

Figure 6.Corrosion rate as a function of the temperature

To determine the regularities of relief and structure formation of zirconium due to thermal influence, metallographic microscopic studies of the surface of the oxidized specimens have been performed. The microstructure of the specimens heated at temperatures of 600, 700 and 900oC after 1860 minute oxidation period are shown on Figures 7, 8 and 9.

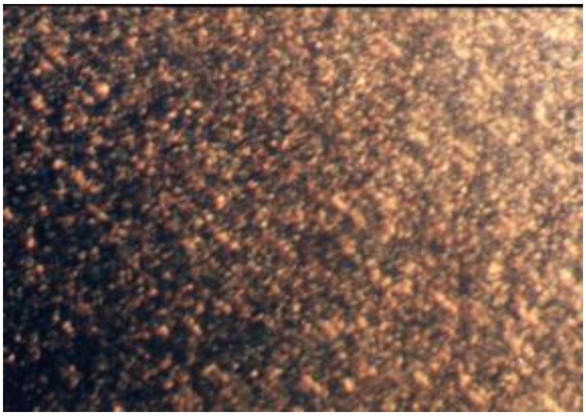

Figure 7. Microstructure of the ZrO_2, x200 T =600°C, t =1860 min

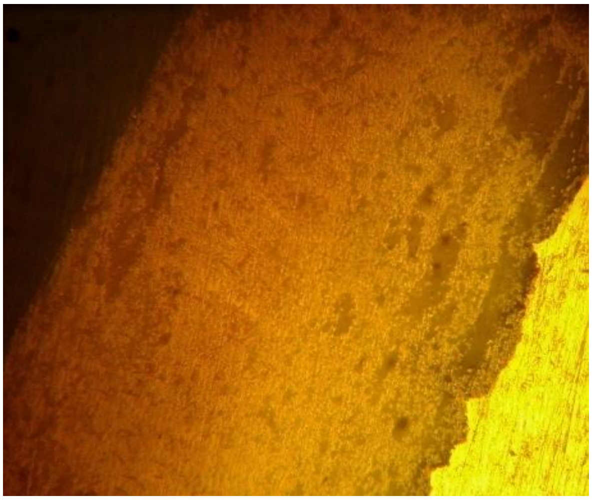

Figure 8. Microstructure of the ZrO_2,x200 T =700 °C, t =1860 min

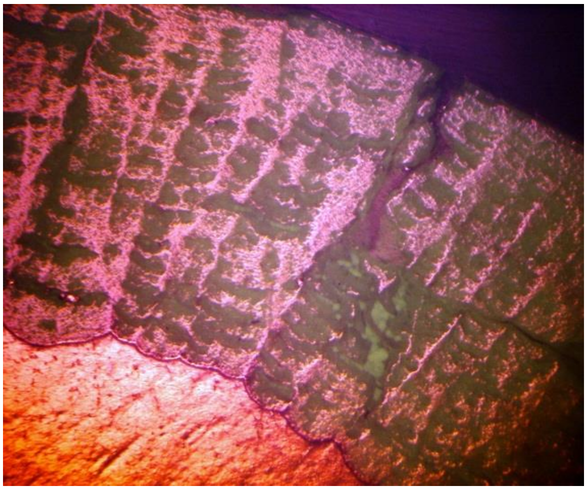

Figure 9. Microstructure of the ZrO_2, x200 T =900°C, t =1860 min

It is well known that zirconium oxide has three well-defined polymorphs: the monoclinic baddeleyite phase, which is stable up to about 1100oC, the tetragonal phase, which appears during annealing treatment up to 1200oC, and the cubic phase, which the compounds adopt at about 2370oC.

Raman spectroscopy is one of the most useful characterization tools because of its non-destructive nature. The Raman spectra for Zr at room temperature and for the heat-treated Zr at 500 and 800oC are presented in Figure 10.

The band appears at wave numbers; 180, 191, 224, 306, 336, 349, 383, 477, 501, 538, 560, 616, 640 and 760 cm-1, which are characteristic for the monoclinic phase.

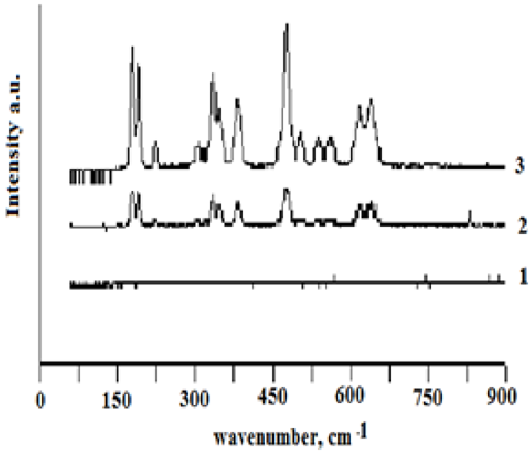

Figure 10. Raman spectra of ZrO_2 formed for exposure time of 30 min at different temperatures 1 - 25°C, 2 – 500°C, 3 – 800°C

4. CONCLUSIONS

The oxidation rate of the zirconium oxidized in air atmosphere is increasing with the increase of the temperature and the exposure time. Initially, the oxidation follows a parabolic rate at all temperatures.

At higher exposure times, at temperatures 700, 800 and 900°C, as a result of the breakaway (loss of protectiveness of the oxide layer), the growth rate of the oxide becomes irregular. The increase of the oxidation rate, which is observed at the breakaway, at temperatures of 700, 800 and 900°C, is mainly due to the ingress of the oxidant down the cracks in the oxide, which then leads to a rapid oxidation. The oxides formed at temperatures of 500 and 600°C are compact for all oxidation times. At higher temperatures, the weight gain (thickness) of the oxide film is increased. At these temperatures, at higher exposure times, cracks appear.

The calculated activation energy of the oxidation reaction is 129.5 kJ/mol.

The Raman spectra for the oxides are characteristic for the monoclinic phase.

REFERENCES

1. Nilson Oliveira T.C., Biaggio S.R., Rocha-Filho R.C. , and Bocchi N., (2002), Studies on the Stability of Anodic Oxides on Zirconium Biocompatible Alloys, J. Braz. Chem. Soc., Vol. 13, No. 4, 463-468.
2. Muktepavela F., Bakradze G., and Stolyarova S., (2007), Nanostructured metal/ oxide coatings, Physica Status Solidi, C 4 (3), 740-743.
3. Subbarao E.C., and Maiti H.S., (1988), Science and technology of zirconia, Advances in Ceramics, Vol. 24, 731–737.
4. Hirvonen A., Nowak R., Yamamoto Y., Sekino T., and Niihara K., (2006), Fabrication, structure, mechanical and thermal properties of zirconia-based ceramic nanocomposites, Journal of the European Ceramic Society, Vol. 26, 8, 1497–1505.
5. Ray J.C., Park D.-W., and Ahn W.-S., (2006), Chemical synthesis of stabilized nano-crystalline zirconia powders, Journal of Industrial and Engineering Chemistry, Vol. 12, 1, 142–148.
6. Gole J.L., Prokes S.M., Stout J.D., Glembock O.J., and Yang R., (2006), Unique properties of selectively formed zirconia nanostructures, Advanced Materials, Vol. 18, 5, 664–667.
7. Dutta G., Hembram K.P., Rao G.M., and Waghmare U.V., (2006), Effects of O vacancies and C doping on dielectric properties of ZrO2, Applied Physics Letters, Vol. 89, 20, Article ID 202904.
8. Garcia J.C., Scolfaro L.M.R., Lino A.T. et al., (2006), Structural, electronic, and optical properties of ZrO2, Journal of Applied Physics, Vol. 100, 10, Article ID 104103.
9. Park S., Vohs J.M. and Gorte R.J., (2000), Direct oxidation of hydrocarbons in a solid-oxide fuel cell, Nature, Vol. 404, 6775, 265–267.
10. Pylypenko M.M., Drobyshevskaya A.A., Stadnik Yu. S. and Tantsyura I.G., (2014), Air-thermal oxidation of zirconium materials, Вопросыатомнойнауки и техники, Vol. 2, 103-106.
11. Koneska Z., (2006), Electrochemical properties of Zirconium in H3PO4 and NaOH solutions, Doctoral thesis, Skopje, Macedonia.
12. Duriez and al., (2008), Zircaloy-4 and M5 high temperature oxidation and nitriding in air, JNM 380, 30-45.
13. Sabol G. P., McDonald S. G., and Airey G. P., (1974), Microstructure of Oxide Films Formed on Zirconium-Based Alloys, Zirconium in Nuclear Applications, 435-448.